Polycyclic bis(amido)cyclodiphosphazane complexes of antimony(III) and bismuth(III): syntheses, molecular structures and solution behaviour

Daniel F. Moser,[a] Ingo Schranz,[a] Michael C. Gerrety,†[a] Lothar Stahl *[a] and Richard J. Staples[b]

[a] Department of Chemistry, University of North Dakota, Grand Forks, ND 58202-9024, USA.
  E-mail: Lothar.Stahl@mail.chem.und.nodak.edu
[b] Department of Chemistry and Chemical Biology, Harvard University, Cambridge,
  MA, 02138, USA

Reactions of $SbCl_3$ and $BiCl_3$ with $[(PNBu^t)_2(NRLi \cdot THF)_2]$ (R = Bu^t, Ph) produced polycyclic cage complexes of the formula $\{[(PNBu^t)_2(NR)_2E]Cl\}$, (E = Sb, R = Bu^t **1a**; E = Bi, R = Bu^t **2**; E = Sb, R = Ph **3**). The bis(*tert*-butylamido)-cyclodiphosphazane complexes of antimony were further derivatized by the substitution of the chloride ligand with N_3 **1b**, -OPh **1c**, and $N(SiMe_3)_2$ **1d** groups. Structural studies showed all compounds to have virtually isometric central polycyclic cages. In solution some of these complexes are fluxional, due to the heavier Group 15 elements pyramidal inversion between two equivalent cyclodiphosphazane ring sites. The activation energies for this process were determined to be a function of both metal and ligand.

While phosphorus amides are a well-known class of inorganic compounds,[1] few analogues of the heavier Group 15 elements exist.[2] This dearth of antimony and bismuth amides is to some extent due to their lesser stability, but it mainly reflects the lack of applications for such compounds. Of the comparatively few metal and metalloid amides of Group 15 which have been reported, most bear simple monodentate ligands,[2] although complexes with chelating ligands have also been synthesized and characterized.[3]

The prospect of using antimony- and bismuth-amido species as precursors for organometallic compounds and solid-state materials has in the recent past rekindled the interest in these complexes.[4] Wright and co-workers, in particular, have shed new light on the reactivity and the structural chemistry of antimony- and bismuth-amido complexes.[5] By using bulky ligands and taking advantage of the structure-controlling lone-pair electrons of these elements in their trivalent state,[6] these chemists have had success in the rational synthesis of heavy Group 15 element amides. Despite these creative approaches, however, many such complexes still suffer from the inherent problems that plague compounds having large metals and monodentate ligands, namely aggregation and lack of control over the metal's steric environment.

We are investigating the use of bis(amido)-substituted inorganic heterocycles as ligands for complexes with predictable geometries and a selective coordination gap. The structure of a bis(amido)cyclodiphosphazane compound of antimony, **1a**[7,8] (Scheme 1), had suggested that this complex's chelating ligand might be useful for the synthesis of well-defined, mono-meric compounds of the heavy Group 15 elements.

Here we report on the syntheses, solid-state structures and solution behaviour of polycyclic bis(amido)cyclodiphosphazane complexes of trivalent antimony and bismuth in which the metal(loid) bears one additional monodentate ligand. In the course of these synthetic studies we also investigated an earlier claim that the fluxionality of **1a** in solution is due to an intermolecular halide exchange.[7]

---

† REU (Research Experience for Undergraduates) participant.

Results

Syntheses

The tricyclic $\{[(PNBu^t)_2(NBu^t)_2]SbCl\}$, **1a**, had originally been synthesized by a trimethylsilylchloride elimination from the reaction of $SbCl_3$ with the amino(imino)phosphine $\{(Bu^tHN)\text{-}P[N(Bu^t)(SiMe_3)]\}$.[7] While this procedure is elegant, its lack of generality and the use of a rather precious phosphine reagent make it costly and time consuming. The bidentate ligand in **1a** is the dianion of the well-known cyclodiphosphazane *cis*-$[(PNBu^t)_2(HNBu^t)_2]$,[10] from which it can be readily generated by treatment with *n*-butyllithium.[11] The interaction of $SbCl_3$ with *cis*-$[(PNBu^t)_2(NBu^tLi \cdot THF)_2]$ (Scheme 1), in turn, offered a much more convenient synthetic route to complexes of this ligand and afforded **1a** in isolated yields of over 90%.

To study the effects of metal(loid), cyclodiphosphazane and monodentate ligand on the structures and stabilities of such complexes, we also synthesized the derivatives $\{[(PNBu^t)_2\text{-}(NBu^t)_2]SbX$, X = N_3 **1b**, OPh **1c**, $N(SiMe_3)_2$ **1d**, $\{[(PNBu^t)_2\text{-}(NBu^t)_2]BiCl\}$ **2**, and $\{[(PNBu^t)_2(NPh)_2]SbCl\}$ **3**. The substitution of chloride with ligands of increasing size, *viz.*, azide, phenoxide and hexamethyldisilazide, was accomplished by treating **1a** with the appropriate alkali-metal salt of the desired ligand, as shown in Scheme 1. All antimony derivatives are colourless compounds that are indefinitely stable under a protective atmosphere of nitrogen or argon.

In notable contrast to the straightforward and high-yielding syntheses of the antimony complexes, the yellow-orange bismuth analogue **2** could be prepared in modest yields of only 30–40%, because of the apparent reduction of the bismuth ion to the metallic state.
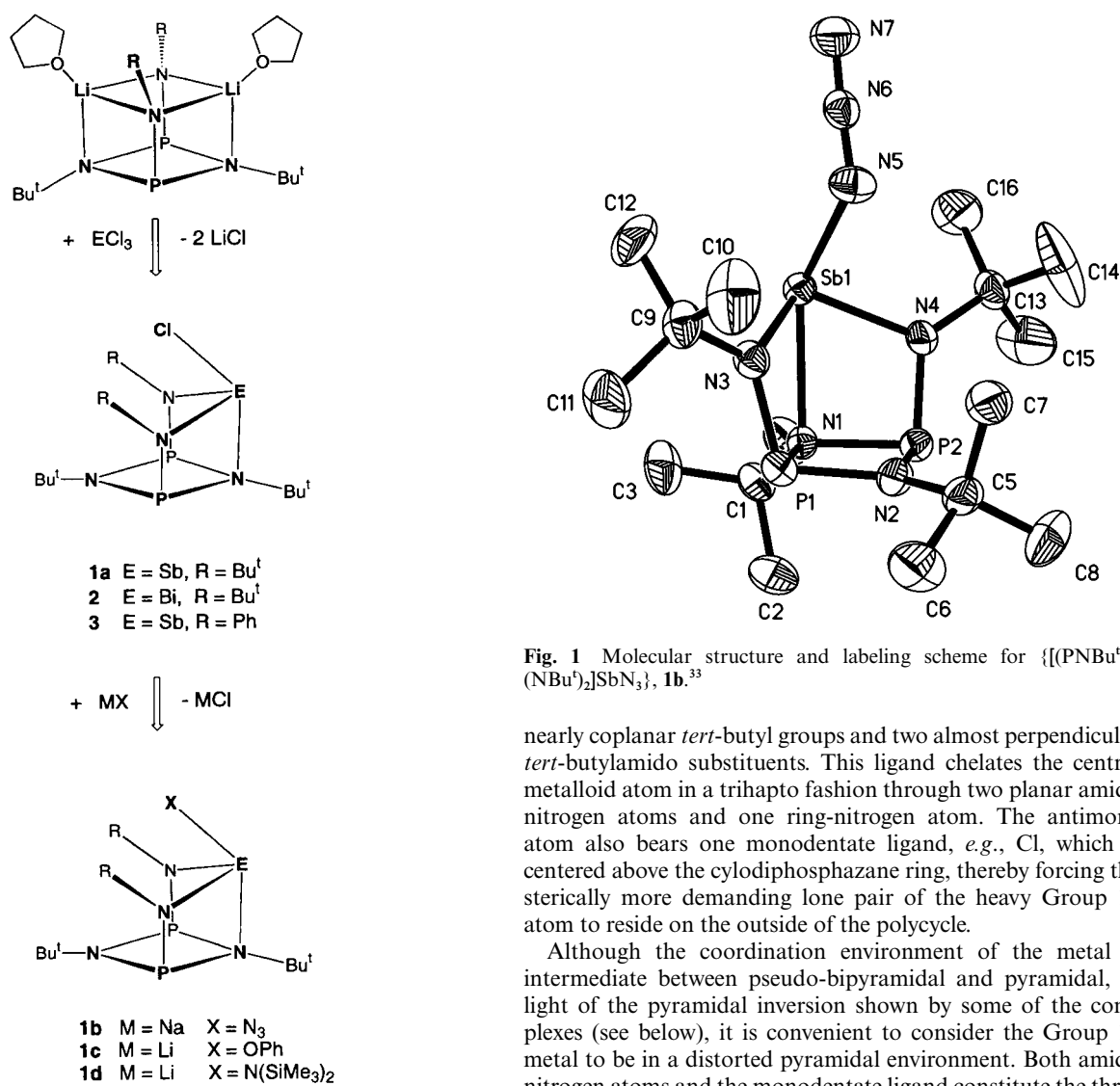
Crystal structures

Tables 1 and 2 contain, respectively, crystal data, and selected bond lengths and angles for the antimony derivatives **1b**–**1d** and **3**. Thermal ellipsoid plots, depicting the solid-state structures of these molecules in a variety of perspectives, are shown in Figs. 1–4. All compounds are highly distorted C_s-symmetric molecular cages, with a planar cylodiphosphazane base (angle

Table 1 Crystal data for compounds **1b**–**1d**, **3**

Compound	1b	1c	1d	3
Formula	$C_{16}H_{36}N_7P_2Sb$	$C_{22}H_{41}N_4OP_2Sb$	$C_{22}H_{54}N_5P_2SbSi_2$	$C_{20}H_{28}N_4ClP_2Sb$
M	510.21	561.28	628.57	543.60
Crystal system	Monoclinic	Monoclinic	Monoclinic	Monoclinic
Space group	$P2_1/c$ (no. 14)	$P2_1/c$ (no. 14)	$P2_1/c$ (no. 14)	$P2_1/n$ (no. 14)
a/Å	9.379(2)	9.548(2)	17.975(3)	11.0596(2)
b/Å	9.621(2)	29.466(6)	10.874(2)	24.5139(2)
c/Å	26.609(6)	19.817(2)	17.765(4)	18.1872(3)
β/°	90.34(2)	90.07(2)	112.67(1)	98.396(1)
U/Å³	2401.0(9)	5575(2)	3204(1)	4878.0(1)
Z	4	8	4	8
F(000)	1048	2320	1320	2192
D_c/Mg m⁻³	1.411	1.337	1.303	1.480
μ/mm⁻¹	1.297	1.123	1.054	1.385
Max., min. transmission coefficient	0.9423, 0.8290	0.8940, 0.7993	0.9623, 0.8711	0.9318, 0.8409
Crystal size/mm	0.20 × 0.14 × 0.10	0.10 × 0.20 × 0.20	0.10 × 0.15 × 0.2	0.1 × 0.1 × 0.2
θ range for data collection/°	0.77–24.78	1.03–25.00	2.24–24.99	1.40–27.68
Reflections collected	9704	10962	16605	22697
Independent reflections	4068 (R_{int} = 0.0244)	7538 (R_{int} = 0.0582)	5616 (R_{int} = 0.0328)	10036 (R_{int} = 0.0281)
$R(F)^a$	0.0326	0.0644	0.0299	0.0288
$wR2(F^2)^b$	0.0773	0.1171	0.0605	0.0655
Weighting factors x, y	0.0171, 8.2598	0, 29.4947	0.0188, 3.0653	0.0326, 0
ρ/e Å⁻³	0.511, −0.559	0.567, −0.547	0.649, −0.333	0.957, −0.717

^{a} $R = \Sigma|F_o - F_c|/\Sigma|F_o|$. ^{b} $wR2 = \{[\Sigma w(F_o^2 - F_c^2)^2]/[\Sigma w(F_o^2)^2]\}^{\frac{1}{2}}$; $w = 1/\sigma^2(F_o)^2 + (xP)^2 + yP]$ where $P = (F_o^2 + 2F_c^2)/3$.

Scheme 1

Fig. 1 Molecular structure and labeling scheme for {[(PNBuᵗ)₂-(NBuᵗ)₂]SbN₃}, **1b**.[33]

nearly coplanar *tert*-butyl groups and two almost perpendicular *tert*-butylamido substituents. This ligand chelates the central metalloid atom in a trihapto fashion through two planar amido nitrogen atoms and one ring-nitrogen atom. The antimony atom also bears one monodentate ligand, *e.g.*, Cl, which is centered above the cylodiphosphazane ring, thereby forcing the sterically more demanding lone pair of the heavy Group 15 atom to reside on the outside of the polycycle.
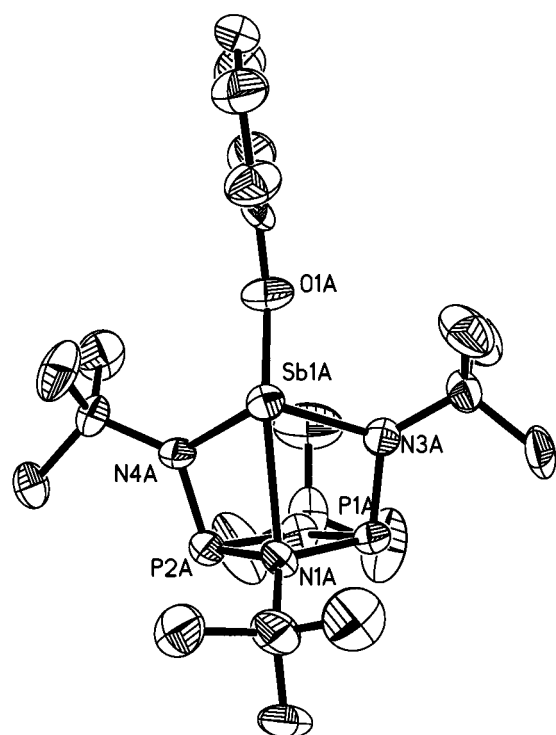
Although the coordination environment of the metal is intermediate between pseudo-bipyramidal and pyramidal, in light of the pyramidal inversion shown by some of the complexes (see below), it is convenient to consider the Group 15 metal to be in a distorted pyramidal environment. Both amido nitrogen atoms and the monodentate ligand constitute the three principal substituents of the metal, while a donor interaction with the cyclodiphosphazane ring forms a weak, fourth bond.

The nearly isometric structures of compounds **1a**–**1c** and the constancy of their nitrogen–antimony bonds prove that the

sum = 359°) and a polycyclic core, which is composed entirely of Group 15 elements. The (P–N)₂ ring is substituted with two

Table 2 Selected bond lengths (Å) and angles (°) for **1a–d** and **3**

	1a	1b	1c	1d	3
Sb–X	2.492(3)	2.199(4)	2.031(8)	2.099(2)	2.439(1)
Sb–N(3)	2.100(6)	2.069(4)	2.104(8)	2.123(2)	2.084(2)
Sb–N(4)	2.089(4)	2.078(4)	2.080(8)	2.120(2)	2.093(2)
Sb–N(1)	2.431(5)	2.421(4)	2.472(8)	2.656(2)	2.490(2)
P(1)–N(1)	1.772(6)	1.777(4)	1.756(8)	1.749(3)	1.778(2)
P(2)–N(1)	1.771(6)	1.780(4)	1.756(8)	1.752(3)	1.769(2)
P(1)–N(2)	1.719(4)	1.717(4)	1.739(8)	1.728(3)	1.716(2)
P(2)–N(2)	1.719(4)	1.721(4)	1.706(8)	1.730(3)	1.718(2)
P(1)–N(3)	1.680(5)	1.683(4)	1.666(8)	1.685(3)	1.693(2)
P(2)–N(4)	1.680(5)	1.679(4)	1.695(8)	1.686(3)	1.706(2)
N(5)–N(6)		1.196(6)			
N(6)–N(7)		1.145(6)			
N(5)–Si(1)				1.749(3)	
N(5)–Si(2)				1.753(3)	
N(3)–E–N(4)		104.36(14)	102.5(3)	100.43(9)	100.78(8)
N(3)–E–X	95.1(2)	89.7(2)	90.6(3)	102.06(1)	91.61(6)
N(4)–E–X	94.5(2)	91.2(2)	90.5(3)	99.55(10)	90.85(6)
N(1)–P(1)–N(2)		80.8(2)	80.1(4)	82.58(12)	81.16(10)
N(1)–P(2)–N(2)		80.7(2)	80.7(4)	82.44(12)	81.40(10)
P(1)–N(1)–P(2)		96.8(2)	98.0(5)	96.59(13)	96.43(10)
P(1)–N(2)–P(2)		101.4(2)	100.9(4)	98.25(13)	100.76(11)
N(3)–P(1)–N(1)		91.4(2)	93.5(4)	95.55(13)	92.01(10)
N(3)–P(1)–N(2)		108.0(2)	106.8(4)	103.77(13)	106.59(11)
N(4)–P(2)–N(2)		107.8(2)	106.4(4)	104.34(13)	106.47(11)
N(4)–P(2)–N(1)		91.8(2)	92.9(4)	95.15(12)	91.40(11)
P(1)–N(1)–E		91.5(2)	90.7(3)	88.22(10)	91.16(8)
P(2)–N(1)–E		91.4(2)	91.3(3)	88.22(10)	92.01(8)
N(3)–E–N(1)		66.43(14)	66.4(3)	63.15(9)	65.50(7)
N(4)–E–N(1)		66.54(14)	65.4(3)	63.04(9)	65.05(7)
Sb–N(5)–N(6)		117.3(3)			
Sb–N(5)–Si(1)				127.04(14)	
Sb–N(5)–Si(2)				112.58(13)	
Si(1)–N(5)–Si(2)				120.36(14)	

Fig. 2 Molecular structure and partial labeling scheme for one of the independent molecules of {[(PNBu^t)$_2$(NBu^t)$_2$]SbOPh}, **1c**.[33]
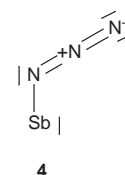
monodentate ligand has little effect on the dimensions of the polycyclic core of the molecule.

This is aptly demonstrated by the structure of the azide derivative **1b**, shown in Fig. 1, whose comparatively small pseudo-halide ligand makes it appear nearly identical with the monochloro complex **1a**. The almost linear (175.8°) triatomic azide unit, whose N(6)–N(5)–Sb moiety encloses an angle of 117.3(3)°, is perpendicularly centered above the cyclodiphosphazane ring. As with similar C_s-symmetric cyclodiphosphazane complexes,[12] the endocyclic P–N bonds are decidedly asymmetric, while the slightly splayed exocyclic P–N bonds have identical lengths. These exocyclic nitrogen atoms form two short, equidistant, 2.069(4) Å and 2.078(4) Å, amide bonds with the antimony atom. A long N–Sb donor bond from the ring-nitrogen atom, 2.421(4) Å, and a comparatively long antimony–azide bond, 2.199(4) Å, complete the coordination sphere of the metalloid.

Experimentally determined E–N$_3$ distances in the related azide complexes {[Te(N$_3$)$_3$]SbF$_6$}[13] 1.994(6) Å, {(PPh$_4$)$_4$-[Sn(N$_3$)$_6$]}[14] 2.150(4) Å, and [CF$_3$As(N$_3$)$_2$][15] 1.862(3) Å, as well as the calculated Sb–N$_3$ bond lengths in [Sb(N$_3$)$_3$][16] 2.045 Å, are all significantly shorter than the antimony–azide bond in **1b**. It is likely that steric repulsions between the azide moiety and the lone-pair electrons of the nitrogen atoms N(3), N(4), and N(2) are responsible for the long Sb–N$_3$ bond in this molecule.

Although the N(5)–N(6) and N(6)–N(7) bonds exhibit a typical long–short pattern, they are more equal in length than in similar molecular azides.[17] In valence-bond terms, the bonding may be presented as shown in **4**, *viz.*, with two double bonds.

4

The X-ray structure determination of the phenoxide derivative **1c** (Fig. 2) was nonroutine, because the data had been collected on a twinned crystal. Owing to these crystallographic
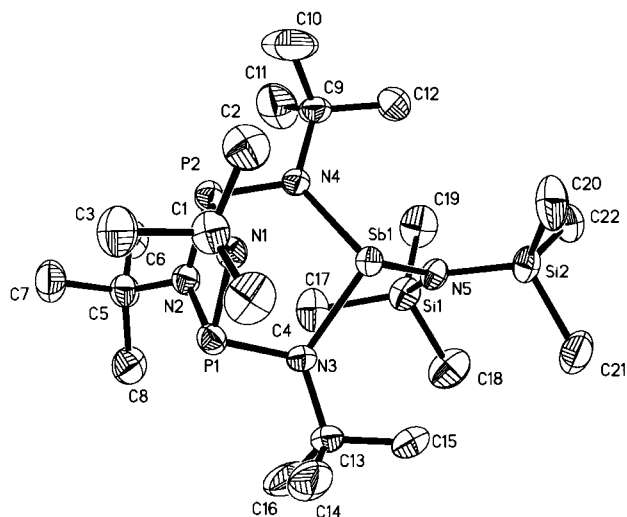
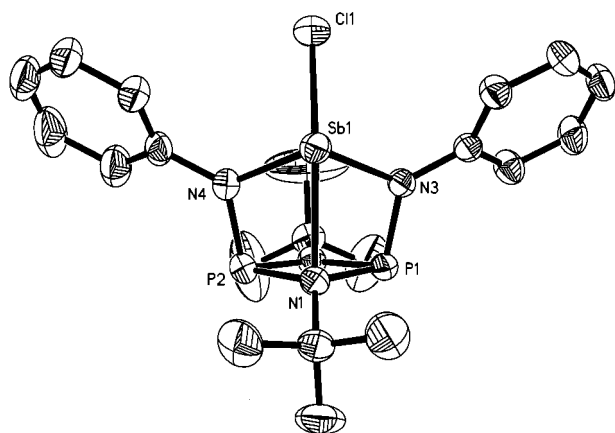**Fig. 3** Molecular structure and labeling scheme for {[(PNBu^t)$_2$-(NBu^t)$_2$]SbN(SiMe$_3$)$_2$}, **1d**.[33]

Fig. 4 Molecular structure and partial labeling scheme for one of the independent molecules of {[(PNBu^t)$_2$(NPh)$_2$]SbCl}, **3**.[33]

problems, the bond parameters of this complex were afflicted with greater uncertainties than those of its analogues. The derived bond lengths and angles, however, are still of sufficient quality for meaningful numerical comparisons.

The phenoxide ligand, whose rather large Ph–O–Sb angle of 124° reflects an sp^2-hybridized oxygen atom, assumes a position in the cleft created by the two *tert*-butylamido substituents, above the center of the cyclodiphosphazane ring. The antimony–oxygen bond, 2.031(8) Å, is of similar length to those in related antimony alkoxides. Thus, for example, the Sb–O bond for the bridging ethoxide ligand in [SbCl$_2$(NHMe$_2$)-(μ-OEt)]$_2$ is 2.005(4) Å long,[18] while the Sb–O bond lengths in an antimony–*o*-quinone complex are 1.994(6) and 2.033(6) Å.[19]

Fig. 3 shows an ORTEP diagram of the hexamethyldisilazide derivative **1d** that emphasizes the perfectly planar coordination environment of the monodentate ligand's nitrogen atom. The presence of this bulky substituent, whose size rivals that of the cyclodiphosphazane moiety, has resulted in a number of structural features that set this complex apart from its analogues. The most obvious of these differences is the substantially longer nitrogen–antimony donor bond, 2.656(2) Å *vs.* 2.411(3) Å, which is due to nonbonding interactions between the bulky *tert*-butyl and trimethylsilyl groups. The Sb–N bond linking the antimony atom and the hexamethyldisilazide ligand, by contrast, is of normal length and *ca.* 0.1 Å shorter than the antimony–azide bond.

The results of an X-ray crystallographic study of the bismuth complex {[(PNBu^t)$_2$(NBu^t)$_2$]BiCl} **2**, are not of sufficient qual-

Table 3 Activation energies for **1a**–**1d**, **2** and **3**
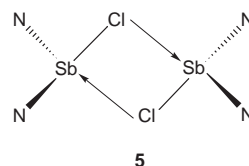
	1a	1b	1c	1d	2	3
E_a/kJ mol^{-1}	>100	>100	>100	>100	53.6	77.4

ity for publication, but they do show the molecule to be a structural analogue of **1a**. It is possible that the disorder problems, which prevented a satisfactory refinement of this complex, reflect the comparatively low barrier to inversion of this complex (see below).

Although the overall structures of the two chloro complexes, **1a** and **3**, are similar, the shorter Sb–Cl and Sb–N donor bonds of the bis(anilido) complex are noteworthy exceptions. A perspective drawing of the highly symmetrical **3** (Fig. 4) shows that the bis(anilido)cyclodiphosphazane[20] ligand has expanded the cyclic theme of these complexes to produce a molecule with three fused inorganic heterocycles that are substituted with two phenyl rings. There are two independent molecules in the monoclinic unit cell, whose structures differ only in the relative orientation of both phenyl groups with respect to each other. One molecule, shown in Fig. 4, has symmetrically disposed phenyl rings, thus maintaining the overall mirror symmetry of the molecule, while in the second molecule one of the phenyl moieties is rotated approximately 90° about the N–phenyl bond from a symmetrical disposition. The frontal view of this molecule pinpoints the lesser steric bulk of the phenyl substituent as the probable cause for the shorter Sb–N and Sb–Cl bonds in this complex.

VT-NMR Studies

We were skeptical of the assertion that the fluxional solution behaviour of **1a** was the result of an intermolecular halide exchange, as shown in **5**.[7] Given the steric crowding about the Sb–Cl bond, such an intermediate seemed unlikely, and we decided to reinvestigate the fluxionality of this complex.

5

The ORTEP drawings of **1b**–**1d** and **3** show that the off-centre location of the metalloid renders the *tert*-butylimido groups of the cylodiphosphazane ring diastereotopic. Room-temperature ^{1}H NMR spectra, which exhibit these groups as two distinct peaks in a 1:1 ratio, prove that this is also the ground-state configuration in solution. On heating to 91 °C, the *tert*-butylimido signals of the bis(anilido) complex **3** coalesced, but those of **1a**–**1d** showed no major changes up to 110 °C.

By contrast, the ambient-temperature ^{1}H NMR spectrum of the bismuth complex, **2**, exhibited only one signal for the ring *tert*-butyl substituents. This peak coalesced at 4 °C and on further cooling reappeared as two distinct singlets, similar to those observed for **1a**–**1d** and **3**. Contrary to earlier reports none of these spectra showed any concentration-dependent dynamic phenomena.[7] From the coalescence temperature and the chemical shift differences of these two peaks, we were able to estimate activation energies for the dynamic behaviour, and these values are summarized in Table 3.
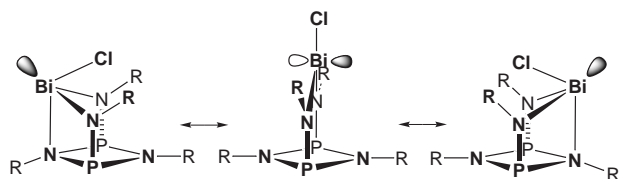
Based on their energies of activation, the complexes can be divided into three groups, *viz.*, (i) the bis(*tert*-butylamido)cyclodiphosphazane complexes of antimony with chloro and monodentate N- and O-donor ligands which show no coalescence up to 110 °C, (ii) the chlorobis(anilido)cyclodiphosphazane antimony species, whose *tert*-butylimido signals coalesced at

91 °C and (iii) the chlorobis(*tert*-butylamido)cyclodiphosphazane bismuth complex, whose NMR signals coalesced below room temperature.

Discussion

The treatment of antimony and bismuth trichlorides with dilithio bis(amido)cyclodiphosphazane species is a convenient synthesis for polycyclic molecules with Group 15 element cores. The ensuing monomeric chlorobis(amido)cylodiphosphazane complexes can be further derivatized by the substitution of the chloride ligand with monodentate N- and O-donor ligands. All compounds are thermally stable and the antimony derivatives can be sublimed *in vacuo* at comparatively low temperatures. In their ground states these tricyclic molecules have idealized C_s-symmetric structures in which the heavy Group 15 element resides above one of the ring nitrogen atoms. This location renders the *tert*-butyl substituents of the imino-nitrogen atoms diastereotopic, resulting in two NMR signals.

Some of these molecules exhibit bond fluctuations, but the absence of concentration-dependent dynamic effects rules out an intermolecular ligand exchange as the cause of the fluxionality and leaves an intramolecular site exchange as the only plausible alternative. A pyramidal inversion, shown in Scheme 2, in

Scheme 2 Pyramidal inversion of the bismuth atom within the cage complex.

which the metal(loid) swings through the central molecular plane is the most likely mode of equilibration. Similar observations were made in a study on related bis(amido)cyclodisilazane complexes, although neither structural details nor activation energies were given.[21]

It is reasonable to assume that bulky organic substituents on the amido nitrogen atoms impede the inversion of the metalloid, and this is indeed corroborated by the VT-NMR studies. These data show the activation energy for the inversion of the bis(anilido)cyclodiphosphazane complex **3** to be at least 22 kJ mol^{-1} lower than that of the sterically more encumbered **1a**. But lack of coalescence of the *tert*-butylimido signals for **1a**–**1d** at attainable temperatures prevented us from assessing the relative steric importance of the monodentate ligand on the pyramidal inversion. Based on the chemical shift differences of the diastereotopic *tert*-butyl groups one can estimate a lower limit of *ca.* 100 kJ mol^{-1} for the inversion barrier in these complexes.

Ligand size, however, is clearly not the sole determining factor for the activation energies, as a comparison of the data for {[(PNBu^t)$_2$(NBu^t)$_2$]SbCl} and {[(PNBu^t)$_2$(NBu^t)$_2$]BiCl} shows. Not only does this isostructural pair of complexes have a fairly large difference in activation energy of *ca.* 50 kJ mol^{-1}, but it is the least sterically hindered complex, namely the one with the smaller metal(loid), that has the higher barrier to inversion. Recent NMR spectroscopic studies on the phosphorus and arsenic analogues of **1a**, suggest inversion barriers of at least 120 kJ mol^{-1}.[22]

The barrier to pyramidal inversion in these cage complexes is thus influenced by both the metal(loid) and the ligand. Based on these rather limited data, we conclude that the activation energy for inversion increases on ascending Group 15. Steric bulk on the chelating ligand also increases the barrier to inversion, but a rigorous discussion of ligand effects is made difficult

by the cyclodiphosphazane's Lewis-basic sites that can, and do, interact with the central metal(loid).

Our results are qualitatively and quantitatively similar to those obtained from experimental and computational investigations on Group 15 compounds of the general type ER$_1$R$_2$R$_3$.[23] A number of such studies have shown that the barrier to pyramidal inversion is a function of central element and ligands. Optically active tertiary amines, for example, rapidly racemize in solution, while the analogous phosphines and arsines, whose barriers to inversion fall in the range 130–180 kJ mol^{-1}, are configurationally stable.[24] Stibines, by contrast, have somewhat lower barriers of *ca.* 110 kJ mol^{-1},[25] and those of bismuthines are presumably lower still.

Conclusion

The title compounds are a homogeneous group of easily synthesized monomeric bis(amido)cyclodiphosphazane derivatives of antimony(III) and bismuth(III), which can be further derivatized to afford a convenient entry into monomeric compounds of these elements. Owing to their unusual coordination geometries these complexes provided the opportunity to obtain activation energies for the pyramidal inversion of heavy Group 15 elements in cage compounds. Although these complexes differ structurally from organic derivatives of antimony and bismuth, their barriers to inversion are surprisingly similar to those of their organometallic counterparts and follow the same group trend.

Experimental

CAUTION: Some azide compounds, especially those having a nitrogen content greater than 25% by weight, are explosive.[26] The antimony azide complex described below, however, showed no tendency to explode; neither on contact nor on heating.

All operations were performed under an atmosphere of argon or prepurified nitrogen on conventional Schlenk lines or in a glove box. The hydrocarbon or ethereal solvents were predried over molecular sieves or CaH$_2$ and distilled under a nitrogen atmosphere from sodium or potassium benzophenone immediately before use. The trichlorides of antimony and bismuth, sodium azide, and lithium phenoxide were purchased from Aldrich and were used as received. Sodium hexamethyldisilazide, provided as a 40% w/w solution in THF, was obtained from Callery Chemical Company, Pittsburgh, PA.

Mass spectra were recorded on a VG Micromass 7070E-HF double-focusing spectrometer in the electron ionization mode, using an accelerating potential of 70 eV, or with a Finnigan MAT 95 in the chemical ionization mode, using methane as the reacting gas. NMR spectra were recorded on a Varian VXR-300 spectrometer. ^{1}H NMR and ^{13}C NMR spectra are referenced relative to C$_6$D$_5$H (δ 7.15) and C$_6$H$_6$ (δ 128.0), respectively. Phosphorus signals are referenced relative to external P(OEt)$_3$ at δ+ 137.0, with shifts to higher frequency (lower field) given a more positive value. Melting points were recorded on a Mel-Temp melting point apparatus; they are uncorrected. E & R Microanalytical Services, Parsippany, NJ, and Robertson Microlit Laboratories, Inc., Madison, NJ performed the elemental analyses. [(Bu^{t}NP)$_2$(Bu^{t}NH)$_2$], and *cis*-[(Bu^{t}NP)$_2$(Bu^{t}NLi·THF)$_2$], were prepared by published procedures.[11]

Syntheses

{[(Bu^{t}NP)$_2$(Bu^{t}N)$_2$Sb]Cl}, 1a. A sample of *cis*-[(Bu^{t}NP)$_2$-(Bu^{t}NLi·THF)$_2$], (4.84 g, 9.60 mmol) dissolved in toluene (25 cm^3) was added dropwise to a toluene solution of antimony trichloride (2.23 g, 9.78 mmol). The initially cloudy, yellow reaction mixture became orange and was stirred overnight at room temperature (RT). Lithium chloride was removed by fil-

tration through a medium-porosity frit and the solution volume was concentrated to *ca.* 4 cm³. After the flask had been stored at −14 ° C for 5 d, colourless crystals of **1a** (4.47 g, 92.6%) were isolated from the solution. Mp 131 °C (decomp.); δ_H (C₆D₆) 1.554 (18 H, s, Buᵗ), 1.378 (18 H, s, Buᵗ), 1.225 (18 H, s, Buᵗ); δ_C (C₆D₆) 57.66 (Me₃*C*), 54.74 (Me₃*C*), 52.69 (Me₃*C*), 33.62 (*Me₃*C), 31.19 (*Me₃*C), 25.85 (*Me₃*C); δ_P (C₆D₆) 157.7.

{[(BuᵗNP)₂(BuᵗN)₂Sb]N₃}, 1b. Solid NaN₃ (0.170 g, 2.61 mmol) was added all at once to **1a** (1.31 g, 2.60 mmol), dissolved in THF (15 cm³). The initially clear solution slowly turned cloudy and was stirred at RT for 16 h. All volatiles were then removed *in vacuo*, and the white residue was dissolved in toluene (5 cm³) and filtered to remove NaCl. This chilled (−14 °C) solution afforded, after several days, colourless, rod-shaped crystals of **1b** (1.10 g, 83.1%). Mp 147 °C (Found: C, 37.50; H, 7.06; N, 19.41. C₁₆H₃₆N₇P₂Sb requires C, 37.67; H, 7.11; N, 19.22%); δ_H (C₆D₆) 1.431 (18 H, s, Buᵗ), 1.349 (9 H, s, Buᵗ), 1.205 (9 H, d, Buᵗ); δ_C (C₆D₆) 56.30 (1 C, d, Me₃*C*), 54.54 (2 C, t, Me₃*C*), 52.71 (1 C, t, Me₃*C*), 33.16 (8 C, d, *Me₃*C), 31.28 (4 C, t, *Me₃*C), 25.80 (4 C, t, *Me₃*C); δ_P (C₆D₆) 155.6; *m/z* (EI, 70 eV) 509.99 (M⁺).

{[(BuᵗNP)₂(BuᵗN)₂Sb]OPh}, 1c. To a sample of **1a** (1.01 g, 2.00 mmol), dissolved in toluene (10 cm³), was added *via* syringe a lithium phenoxide solution (1.0 M, 2.0 cm³). The colourless mixture was stirred for 24 h at RT, filtered through a medium-porosity frit, and concentrated to 2 cm³. After the flask had been stored at −14 °C for several days, colourless plate-shaped crystals of **1c** (0.79 g, 71%) were isolated. Mp 114–116 °C (Found: C, 47.03; H, 7.56; N, 9.81. C₂₂H₄₁N₄OP₂Sb requires C, 47.08; H, 7.36; N, 9.98%); δ_H (C₆D₆) 7.247 (2 H, t, *meta* H), 7.135 (2 H, t, *ortho* H), 6.828 (1 H, t, *para* H), 1.418 (27 H, s, Buᵗ), 1.334 (9 H, s, Buᵗ); δ_C (C₆D₆) 161.2 (1 C, s, arom. C), 129.92 (2 C, s, arom. C), 119.55 (2 C, s, arom. C), 118.73 (1 C, s, arom. C), 56.36 (1 C, d, Me₃*C*), 54.55 (2 C, t, Me₃*C*), 52.75 (1 C, t, Me₃*C*), 33.89 (4 C, d, *Me₃*C), 31.40 (8 C, t, *Me₃*C), 26.11 (4 C, t, Me₃*C); δ_P (C₆D₆) 158.8; *m/z* (EI, 70 eV) 469 (M − OPh).

{[(BuᵗNP)₂(BuᵗN)₂Sb]N(SiMe₃)₂}, 1d. Crystalline **1a** (0.528 g, 1.05 mmol) was dissolved in toluene (15 cm³) in a 100 cm³ two-necked flask, equipped with an inert gas inlet and a magnetic stirring bar. A sodium hexamethyldisilazide solution (15.0 cm³, 0.075 M) was then added dropwise at 0 °C to this solution, and the ensuing reaction mixture was stirred overnight at 50 °C. All volatiles were removed *in vacuo*, and the dry, tan residue was extracted with toluene (10 cm³). The extract was filtered through a medium-porosity frit and concentrated to 4 cm³ *in vacuo*. After the flask had been stored for several days at −14 °C, colourless crystals of **1d** (0.544 g, 82.5%) formed. Mp 259 °C (Found: C, 41.61; H, 8.59; N, 10.72. C₂₂H₅₄N₅P₂Si₂Sb requires C, 42.04; H, 8.66; N, 11.14%); δ_H (C₆D₆) 1.525 (18 H, s, Buᵗ), 1.338 (18 H, s, Buᵗ), 0.659 (9 H, s, SiMe₃), 0.380 (9 H, s, SiMe₃); δ_C (C₆D₆) 58.55 (2 C, d, Me₃*C*), 53.63 (2 C, t, Me₃*C*), 34.90 (6 C, d, *Me₃*C), 29.66 (3 C, t, *Me₃*C), 27.93 (3 C, t, *Me₃*C), 7.34 (3 C, s, SiMe₃), 5.84 (3 C, s, SiMe₃); δ_P (C₆D₆) 155.08; *m/z* (CI, methane) 628.249 (M⁺).

{[(BuᵗNP)₂(BuᵗN)₂Bi]Cl}, 2. To freshly-sublimed bismuth trichloride (3.32 g, 10.53 mmol), dissolved in cold THF (−78 °C, 25 cm³), was added dropwise a toluene solution of [(BuᵗNP)₂(BuᵗNLi·THF)₂] (5.02 g, 10.0 mmol). Upon warming, the orange solution became greenish-black. After 1 d all volatiles were removed *in vacuo*, leaving a yellow-black residue. Extraction of this solid with toluene (20 cm³) afforded, upon filtration, a clear, bright yellow solution, which was concentrated *in vacuo* to 5 cm³. After the flask had been stored at −14 °C for 6 d, hexagonal, orange plates of **2** (1.87 g, 32.0%) were isolated from

the solution. Mp 184 °C (decomp.) (Found: C, 32.57; H, 6.02; N, 9.35. C₁₆H₃₆N₄P₂ClBi requires C, 32.53; H, 6.14; N, 9.48%); δ_H (C₇D₈, 298 K) 1.409 (18 H, s, Buᵗ), 1.297 (18 H, s, Buᵗ); (C₇D₈, 233 K) 1.451 (9 H, s, Buᵗ), 1.421 (18 H, s, Buᵗ), 1.189 (9 H, s, Buᵗ); δ_C (C₆D₆) 56.9 (2 C, d, Me₃*C*), 53.6 (2 C, br, Me₃*C*), 35.25 (6 C, d, *Me₃*C), 29.1 (6 C, br, *Me₃*C); δ_P (C₆D₆) 163.78; *m/z* (CI, methane) 590.1910 (M⁺).

{[(BuᵗNP)₂(NPh)₂Sb]Cl}, 3. In a two-neck flask, equipped with gas inlet and stirring bar, antimony trichloride (0.20 g, 0.88 mmol) was dissolved in cold toluene (10 cm³). A clear, yellow solution of [(BuᵗNP)₂(NPhLi·THF)₂]²⁰ (0.48 g, 0.88 mmol) in toluene (10 cm³) was added dropwise to the cooled (0 °C), antimony trichloride solution. The reaction mixture was stirred overnight at RT, filtered through a medium-porosity frit, and concentrated *in vacuo* until small crystals formed. These crystals were allowed to redissolve, and the flask was then kept at −12 °C for 1 d to afford block-shaped, pale-yellow crystals of **3** (0.41 g, 85%). Mp 150–152 °C (Found: C, 44.34; H, 5.33; N, 10.51; C₂₀H₂₈N₄P₂SbCl requires C, 44.19; H, 5.19; N, 10.31%); δ_H (C₇D₈, 298 K) 7.28 (4 H, d, *ortho* H), 7.21 (4 H, t, *meta* H), 6.92 (2 H, t, *para* H), 1.34 (9 H, s, NBuᵗ), 1.26 (9 H, s, NBuᵗ); δ_C (C₆D₆) 144.7 (s), 129.3 (s), 123.7 (s), 123.4 (s), 54.4 [t, *J*(PC) 11.1], 52.8 [t, *J*(PC) 5.0 Hz], 30.8 (6 C, d, *Me₃*C), 26.3 (6 C, br, *Me₃*C); δ_P (C₆D₆) 169.9.

X-ray crystallography

All crystals were grown from supersaturated toluene solutions at the indicated temperatures. They were coated with Paratone, affixed to a glass capillary, and centered on the diffractometer in a stream of cold nitrogen. Reflection intensities were collected with a Bruker SMART CCD (charge-coupled device) diffractometer, equipped with an LT-2 low-temperature apparatus operating at 193 K. Data were measured using ω scans of 0.3° per frame for 30 seconds until a complete hemisphere had been collected. The first 50 frames were recollected at the end of data collection to monitor for decay; none was observed. Cell parameters were retrieved using SMART²⁷ software and refined with SAINT²⁸ on all observed reflections. Data reduction was performed with SAINT, which corrects for Lp and decay. An empirical absorption correction was applied with SADABS.²⁹ The structures were solved by direct methods with the SHELXS-90³⁰ program and refined by full-matrix least squares methods on F^2 with SHELXL-97,³¹ incorporated in SHELXTL-PC V 5.03.³² The positions of all non-hydrogen atoms were deduced from difference Fourier maps and refined anisotropically. Hydrogen atoms were placed in their geometrically generated positions and refined riding on the carbon atom to which they are attached.

The crystal structure refinement of **1d** was nonroutine, because the crystal was a rotation twin, twin axis [1 0 0]. Although the reflections of both fragments generally could be resolved, a peak-profile analysis showed that a small amount of twin component may have been present in the collected data. In addition, there were two independent molecules in the monoclinic unit cell, each of which was afflicted with a site-disorder for the antimony atom. These problems are reflected in higher residuals and greater statistical uncertainties for the metric parameters of this compound.

CCDC reference number 186/1304.

See http://www.rsc.org/suppdata/dt/1999/751/ for crystallographic files in .cif format.

References

1 See, for example: M. F. Lappert, A. R. Sanger, R. C. Srivastava and P. P. Power, *Metal and Metalloid Amides*, Ellis Horwood, Chichester, 1980; N. N. Greenwood and A. Earnshaw, *Chemistry of the Elements*, Butterworth and Heinemann, Oxford, 2nd edn., 1997; D. E. C. Corbridge, *Phosphorus: An Outline of its Chemistry, Biochemistry and Technology*, Elsevier, Amsterdam, 5th edn., 1995.

2 J. Dahlmann and K. Winsel, *Ger. Pat.*, 83 136, 1971; H. Funk and H. Kohler, *J. Prakt. Chem.*, 1961, **14**, 226; T. A. George and M. F. Lappert, *J. Chem. Soc. A*, 1969, 992; D. Hass, *Z. Chem.*, 1964, **4**, 185; D. Hass and D. Cech, *Z. Chem.*, 1970, **10**, 33; K. Moedritzer, *Inorg. Chem.*, 1964, **3**, 609; N. Kuhn and O. Scherer, *Z. Naturforsch., Teil B*, 1979, **34**, 888; M. Björgvinsson, H. W. Roesky, F. Pauer and G. M. Sheldrick, *Chem. Ber.*, 1992, **125**, 767; F. Ando, T. Hayashi, K. Ohashi and J. Koketsu, *J. Inorg. Nucl. Chem.*, 1975, **37**, 2011; W. Neubert, H. Pritzkow and H. P. Latscha, *Angew. Chem., Int. Ed. Engl.*, 1988, **27**, 287.

3 M. Veith, B. Bertsch and V. Huch, *Z. Anorg. Allg. Chem.*, 1988, **559**, 73; S. K. Pandey, R. Hasselbring, A. Steiner, D. Stalke and H. W. Roesky, *Polyhedron*, 1993, **12**, 2941; A.-M. Caminade, M. Veith, V. Huch and W. Malisch, *Organometallics*, 1990, **9**, 1798.

4 W. Clegg, N. A. Compton, R. J. Errington, N. C. Norman and N. Wishart, *Polyhedron*, 1989, **8**, 1579; W. Clegg, N. A. Compton, R. J. Errington, G. A. Fisher, M. E. Green, D. C. R. Hockless and N. C. Norman, *Inorg. Chem.*, 1991, **30**, 4680.

5 A. J. Edwards, M. A. Paver, P. R. Raithby, M.-A. Rennie, C. A. Russell and D. S. Wright, *Angew. Chem., Int. Ed. Engl.*, 1994, **106**, 1134; A. J. Edwards, N. E. Leadbeater, M. A. Paver, M.-A. Rennie, P. R. Raithby, C. A. Russell and D. S. Wright, *J. Chem. Soc., Dalton Trans.*, 1994, 2963.

6 M. Beswick, M. E. G. Misquera and D. S. Wright, *J. Chem. Soc., Dalton Trans.*, 1998, 2437.

7 O. J. Scherer, G. Wolmershäuser and H. Conrad, *Angew. Chem., Int. Ed. Engl.*, 1983, **22**, 404.

8 Although this complex was unambiguously characterized by single-crystal X-ray analysis and other techniques, it has been misrepresented as {[(PNSiMe₃)₂(NSiMe₃)₂]SbCl} in at least three review articles.⁹

9 E. Niecke, in *Multiple Bonds and Low Coordination in Phosphorus Chemistry*, eds. M. Regitz and O. Scherer, Thieme, Stuttgart, 1990, p. 293; M. Witt and H. W. Roesky, *Chem. Rev.*, 1994, **94**, 1163; E. Niecke and D. Gudat, *Angew. Chem., Int. Ed. Engl.*, 1991, **30**, 217.

10 R. R. Holmes and J. A. Forstner, *Inorg. Chem.*, 1963, **2**, 380; T. G. Hill, R. C. Haltiwanger, M. L. Thompson, S. A. Katz and A. D. Norman, *Inorg. Chem.*, 1994, **33**, 1770.

11 I. Schranz, L. Stahl and R. J. Staples, *Inorg. Chem.*, 1998, **37**, 1493.

12 L. Grocholl, I. Schranz, L. Stahl and R. J. Staples, *Inorg. Chem.*, 1998, **37**, 2496; L. Grocholl, V. Huch, L. Stahl, R. J. Staples, P. Steinhart and A. Johnson, *Inorg. Chem.*, 1997, **36**, 4451; L. Grocholl, I. Schranz, L. Stahl and R. J. Staples, *Chem. Commun.*, 1997, 1465.

13 J. P. Johnson, G. K. MacLean, J. Passmore and P. S. White, *Can. J. Chem.*, 1989, **67**, 1687.

14 D. Fenske, H.-D. Dörner and K. Dehnicke, *Z. Naturforsch., Teil B*, 1983, **38**, 1301.

15 H. W. Ang, W. L. Kwik, Y. W. Lee and H. Oberhammer, *Inorg. Chem.*, 1994, **33**, 4425.

16 T. M. Klapötke, A. Schulz and J. McNamara, *J. Chem. Soc., Dalton Trans.*, 1996, 2985.

17 A. H. Cowley, F. Gabbai, R. Schluter and D. Atwood, *J. Am. Chem. Soc.*, 1992, **114**, 3142.

18 A. J. Edwards, N. E. Leadbeater, M. A. Paver, P. R. Raithby, C. A. Russell and D. S. Wright, *J. Chem. Soc., Dalton Trans.*, 1994, 1479.

19 Z. Tian and D. G. Tuck, *J. Chem. Soc., Dalton Trans.*, 1993, 1381.

20 D. F. Moser and L. Stahl, unpublished results.

21 M. Veith, A. Rammo and M. Hans, *Phosphorus, Sulfur Silicon Relat. Elem.*, 1994, **93–94**, 197.

22 I. Schranz, D. F. Moser and L. Stahl, manuscript in preparation.

23 G. W. Koeppl, D. S. Sagatys, G. S. Krishnamurthy and S. I. Miller, *J. Am. Chem. Soc.*, 1967, **89**, 3396; L. Horner and H. Winkler, *Tetrahedron Lett.*, 1964, 461. R. E. Weston, Jr., *J. Am. Chem. Soc.*, 1954, **76**, 2645.

24 R. D. Baechler and K. Mislow, *J. Am. Chem. Soc.*, 1971, **93**, 773; G. H. Senkler, Jr. and K. Mislow, *J. Am. Chem. Soc.*, 1972, **94**, 291.

25 J. Jacobus, *Chem. Commun.*, 1971, 1058.

26 S. Patai (editor), *The Chemistry of the Azide Group*, Interscience, London, 1971.

27 SMART V 4.043 Software for the CCD Detector System, Bruker Analytical X-ray Systems, Madison, WI, 1995.

28 SAINT V 4.035 Software for the CCD Detector System, Bruker Analytical X-ray Systems, Madison, WI, 1995.

29 SADABS program for absorption corrections using the Bruker CCD Detector System. Based on: R. Blessing, *Acta Crystallogr., Sect. A*, 1995, **51**, 33.

30 G. M. Sheldrick, SHELXS-90, Program for the Solution of Crystal Structures, University of Göttingen, 1990.

31 G. M. Sheldrick, SHELXL-97, Program for the Solution of Crystal Structures, University of Göttingen, 1997.

32 SHELXTL 5.03 (PC-Version), Program Library for Structure Solution and Molecular Graphics, Bruker Analytical X-ray Systems, Madison, WI, 1995.

33 C. K. Johnson, ORTEP, Report ORNL-5138. Oak Ridge National Laboratory, Oak Ridge, TN, 1976.